Three-Dimensional Relativistic Electromagnetic Subcycle Solitons

Timur Esirkepov,[1,*] Katsunobu Nishihara,[1] Sergei V. Bulanov,[2] and Francesco Pegoraro[3]
[1]*Institute of Laser Engineering, Osaka University, 2-6 Yamada-oka, Suita, Osaka 565-0871, Japan*
[2]*Advanced Photon Research Center, JAERI, Kizu-minami, Kyoto-fu 619-0215, Japan*
[3]*University of Pisa and INFM, via Buonarroti 2, Pisa 56100, Italy*
(Received 9 May 2002; published 17 December 2002)

Three-dimensional (3D) relativistic electromagnetic subcycle solitons were observed in 3D particle-in-cell simulations of an intense short-laser-pulse propagation in an underdense plasma. Their structure resembles that of an oscillating electric dipole with a poloidal electric field and a toroidal magnetic field that oscillate in phase with the electron density with frequency below the Langmuir frequency. On the ion time scale, the soliton undergoes a Coulomb explosion of its core, resulting in ion acceleration, and then evolves into a slowly expanding quasineutral cavity.

DOI: 10.1103/PhysRevLett.89.275002 PACS numbers: 52.35.Sb, 42.65.Tg, 52.27.Ny, 52.65.Rr

Time evolution of a three-dimensional (3D) nonlinear wave, in general, differs drastically from that of 1D or 2D waves, as exemplified by the problems of the wave collapse [1] and of the transverse stability of solitons [2]. Relativistic electromagnetic solitons are now routinely observed in 2D particle-in-cell (PIC) simulations [3–6] in the wake of an intense short laser pulse propagating in an underdense plasma. Solitons attract great attention because they are of fundamental importance for nonlinear science [7] and are considered to be a basic component of turbulence in plasmas [8]. Thus, the numerical identification of solitons, among the different kinds of coherent structures that are formed by an intense laser pulse in a plasma, stimulated a renewed interest in developing an analytical model [9,10] and in envisaging ways of detecting solitons experimentally [11].

As was stressed in Ref. [12], a detailed description of the strong electromagnetic wave interaction with plasmas represents a formidable difficulty for analytical methods, due to the high dimensionality of the problem, the lack of symmetry, and the importance of nonlinear and kinetic effects. On the other hand, powerful methods for investigating the laser-plasma interaction have become available through the advent of modern supercomputers. In the case of an ultrashort relativistically strong laser pulse, simulations with 3D PIC codes provide a unique opportunity for describing the nonlinear dynamics of laser plasmas adequately, including the generation of coherent nonlinear structures, such as the relativistic solitons. In this Letter, we present numerical identification of a 3D subcycle relativistic soliton and complex spatial structure of its electromagnetic fields.

Briefly summarizing the recent results in the analytical and numerical investigation of relativistic solitons in plasmas, we recall the development of the analytical theory of intense electromagnetic solitons [9,10,13] (see also references in Ref. [14]). The solitons found in 1D and 2D simulations consist of slowly or nonpropagating electron density cavities inside which an electromagnetic field is trapped and oscillates coherently with a frequency below the unperturbed plasma frequency and with a spatial structure corresponding to half a cycle. One-dimensional subcycle relativistic electromagnetic solitons in an underdense plasma were observed for the first time in a PIC simulation in Ref. [15], where the mechanism of soliton formation and the structure of the circularly polarized soliton were investigated. The mechanism of soliton formation is related to the fact that the frequency in the rear part of an intense laser pulse propagating in an underdense plasma decreases down to the local Langmuir frequency because the pulse loses its energy while the number of photons is conserved. As a result, the low-frequency part of the electromagnetic radiation of the pulse, propagating with very low velocity, is trapped inside the cavity in the electron density, and a subcycle soliton is formed. An exact analytical solution of the electron fluid-Maxwell equations representing 1D circularly polarized relativistic electromagnetic subcycle soliton was obtained in Ref. [9] in perfect agreement with 1D PIC simulations. The 2D relativistic electromagnetic subcycle solitons discovered in the PIC simulations [3] consist of two "pure" types of solitons: *S* solitons with transverse electric field and azimuthal magnetic field with respect to the symmetry axis, and *P* solitons with the opposite structure: transverse magnetic field and azimuthal electric field. In contrast to electron vortices, which move across a density gradient, solitons move along the density gradient towards the lower density. When a soliton reaches some critical density, it radiates its energy in the form of a low-frequency short electromagnetic burst [4]. The interaction of two 2D *S* solitons leads to their merging, and the resulting soliton acquires the total energy of the two merged solitons [16]. Moreover, in an electron-ion plasma, a 2D soliton evolves into a postsoliton [6] on an ion time scale due to the ion acceleration caused by the time-averaged electrostatic field inside the soliton. This effect leads to the formation of slowly expanding bubbles in the plasma density [6].

Note that here we use the term "soliton" for brevity, even if, in principle, the merging and the expansion on the ion time violate the strict definition of these structures as solitons.

We present the results of a three-dimensional simulation of a laser induced subcycle relativistic electromagnetic soliton. We use the REMP—relativistic electromagnetic particle—mesh code based on the particle-in-cell method. This parallel and fully vectorized code exploits a new scheme of current assignment [17] that reduces unphysical numerical effects of the PIC method significantly. In the simulation, the laser pulse propagates along the x axis. The pulse is linearly polarized in the direction of the z axis and its dimensionless amplitude is $a = eE_z/(m_e\omega c) = 1$, corresponding to the peak intensity $I = 1.38 \times 10^{18}$ W/cm^2 for the $\lambda = 1$ μm laser. The laser pulse has a Gaussian envelope with FWHM size $8\lambda \times 5\lambda \times 5\lambda$. Its focal plane is placed in front of the plasma slab at the distance of 3λ. The length of the plasma slab is 13λ. The plasma density is $n_e = 0.36n_{\rm cr}$. Ions and electrons have the same absolute charge, and the mass ratio is $m_i/m_e = 1836$. The simulation box has $660 \times 400 \times 400$ grids with a mesh size of 0.05λ. The total number of quasiparticles is 426×10^6. The boundary conditions are periodic along the y and z axes and absorbing along the x axis for both the EM radiation and the quasiparticles. The simulations were performed on 16 processors of the NEC SX-5 vector supercomputer in Cybermedia Center, Osaka University. The simulations results are shown in Figs. 1–5, where the space unit is the wavelength λ of the incident radiation.

In Fig. 1, we see one isolated soliton and a soliton train behind the laser pulse. A substantial part of the laser energy (up to 30%) is transformed into these coherent entities. Figures 2 and 3 show the structure of the isolated soliton with the electric and magnetic fields and the electron density at two different times with the interval approximately half of a soliton oscillation period. In the figures, the space unit is the wavelength λ of the incident laser pulse. The soliton consists of oscillating electrostatic and electromagnetic fields confined in a prolate cavity of the electron density. The cavity size is approximately $2\lambda \times 2\lambda \times 3\lambda$. The cavity is generated by the ponderomotive force and the resulting charge separation induces a dipole electrostatic field. As seen in Fig. 2, the charge density in the soliton oscillates up and down in the z direction: at $\omega t/2\pi = 39.3$, the electron hole is in the upper part of the figure and the electron hump is in the lower, and vice versa—at $\omega t/2\pi = 40.2$. The electric field at the soliton center is perpendicular to the direction of the laser propagation, so this mode differs from the laser-driven plasma wake. This field is so large that the quivering distance of electrons in the z direction is of the order of the cavity size. This in turn results in continuous oscillations of the cavity. The soliton resembles an oscillating electric dipole. The oscillating toroidal magnetic field, shown in Fig. 3, indicates that, besides the strong electrostatic field, the soliton also has the electromagnetic field. The electrostatic and electromagnetic components in the soliton are of the same order of magnitude.

Figure 3 shows that the electric field in the soliton is poloidal, while the magnetic field is toroidal. We note that the magnetic field is mostly counterclockwise in the upper part of the soliton, and clockwise in the lower part. This structure of the electromagnetic field can be considered as that of the lowest eigenmode of a cavity resonator with a deformable wall, and thus we call this structure a transverse magnetic (TM) soliton. Figure 4 shows the z component of the normalized electric field at the center of the soliton. The electromagnetic field trapped in the

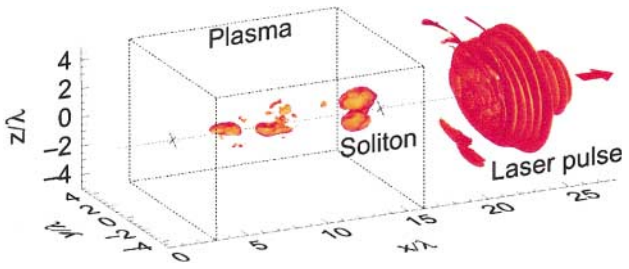

FIG. 1 (color). Isosurface of electromagnetic energy density corresponding to dimensionless value of $(E^2 + B^2)/8\pi = 0.09/8\pi$ at $t = 33.75 \times 2\pi/\omega$.

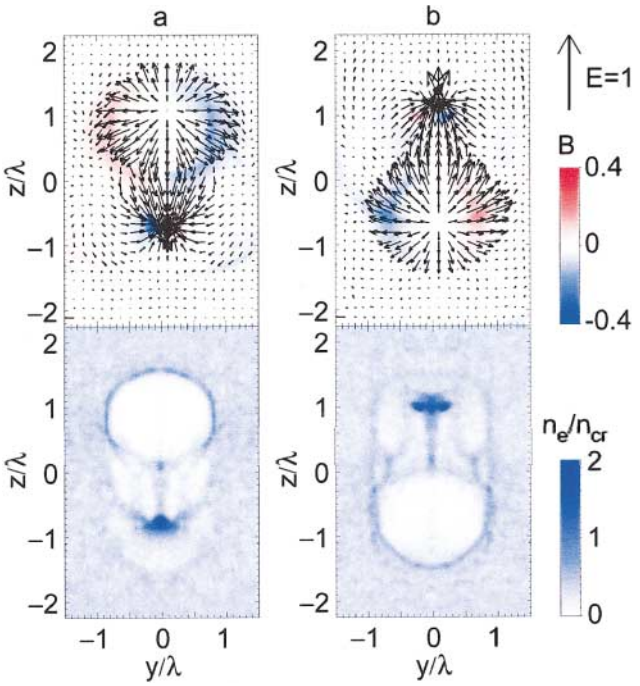

FIG. 2 (color). Soliton structure in the y-z plane at $x = 14.5$. In the upper row, arrows represent electric field, E_y and E_z, where arrow length in the right of the figure corresponds to $eE/m_e\omega c = 1$, and background color indicates magnetic field $eB_x/m_e\omega c$. In the bottom row, electron density is shown with brightness scale. (a) corresponds to $t = 39.3 \times 2\pi/\omega$ and (b) $t = 40.2 \times 2\pi/\omega$.

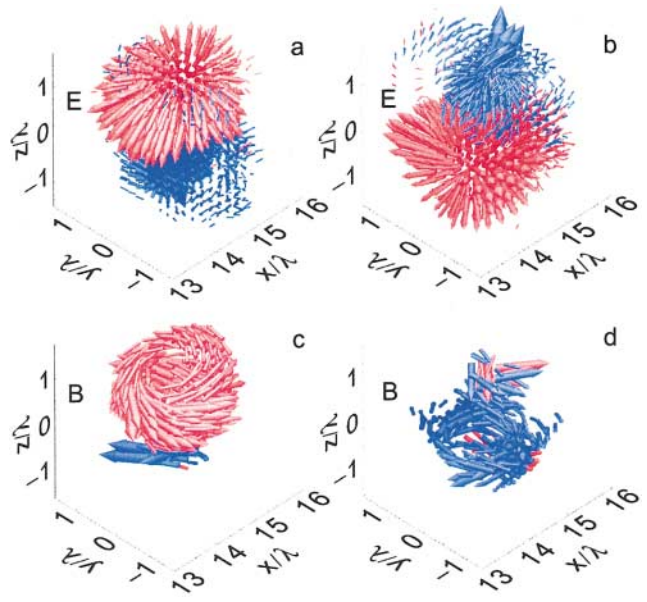

FIG. 3 (color). Three-dimensional structure of electric field [(a),(b)] and magnetic field [(c),(d)] in the soliton corresponding to Fig. 2. In the electric field red and blue denote positive and negative values of its divergence. In the magnetic field red and blue denote counterclockwise and clockwise rotation. Arrows' length corresponds to the magnitude of the fields. Frames (a) and (c) correspond to $t = 39.3 \times 2\pi/\omega$; (b) and (d) to $t = 40.2 \times 2\pi/\omega$.

oscillating cavity pulsates at the same frequency Ω_S that is smaller than the surrounding unperturbed Langmuir frequency, $\Omega_S \approx 0.87\omega_{pe}$. The density of the cavity walls is $(2–3)n_{\rm cr}$. Therefore the electromagnetic energy cannot be radiated away, and, in addition, the soliton oscillation does not resonate with plasma waves.

In the equatorial plane, the structure of the three-dimensional soliton is similar to that of a two-dimensional S soliton, while that in the perpendicular planes is similar to a two-dimensional P soliton. Considering the soliton as a wave packet, it has only half of one cycle in space, so we use the term "subcycle soliton." The dynamic of the 3D soliton is clearly seen in the animations produced from the data (420 stills with period 0.05, see authors' Web site). Although as shown in Fig. 4 the field amplitude inside the soliton decreases because of its energy losses due to ion acceleration and

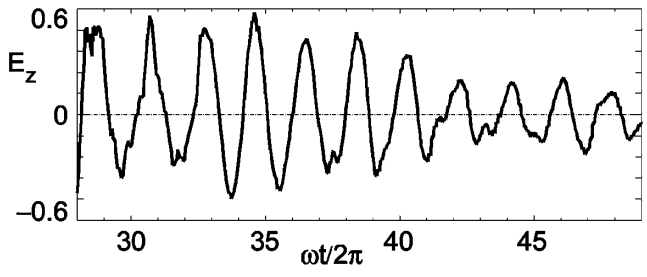

FIG. 4. Time dependence of the z component of electric field, $eE_z/m_e\omega c$, at the center of the soliton, $(x, y, z) = (14.5, 0, 0)$.

to the digging of a hole in the ion density as discussed below, the soliton lifetime is sufficiently long to distinguish it from the other nonlinear modes generated by the laser pulse, such as the pulse wakefield or vortices.

On the ion time scale, the soliton evolves into a postsoliton [6]. The ponderomotive force displaces the electrons outward and the Coulomb repulsion in the electrically non-neutral ion core pushes the ions away with a process similar to the Coulomb explosion. The evolution of the wave-plasma interaction discussed can also be interpreted as a phenomenon similar to the wave collapse that is, however, saturated because the electrons are almost completely evacuated by the strong wave. As the soliton amplitude decreases, the ions acquire a radial momentum, as shown in Fig. 5. In contrast to the 2D S-polarized soliton discussed in Ref. [6], the explosion of the 3D TM soliton is strongly anisotropic (the postsoliton cavity is elongated in the z direction) and the energy spectrum of the accelerated ions has a minimum at zero. In Fig. 5, we see also the ion implosion near the center of the postsoliton. The ion implosion may appear in the postsoliton regime due to the electron heating by the trapped electromagnetic field at the density cavity walls, which causes the plasma ablation towards the cavity center similar to the ion implosion and the dense plasma filament formation at the axis of the self-focusing channel discussed in Ref. [18].

At the last stage of the soliton evolution, we see a slowly expanding postsoliton where the walls of the plasma cavity move with velocity $v \approx 3 \times 10^{-3}c$. We notice that in the case of immobile ions we also see the soliton formation, but the lifetime of the soliton is significantly longer and is determined by energy conversion into fast electrons similar to Landau damping. The almost isolated structures in the soliton train, which we consider as solitons even if they are not properly separated, tend to merge and form a foam of bubbles with relatively high density ($\approx 3n_{\rm cr}$) walls.

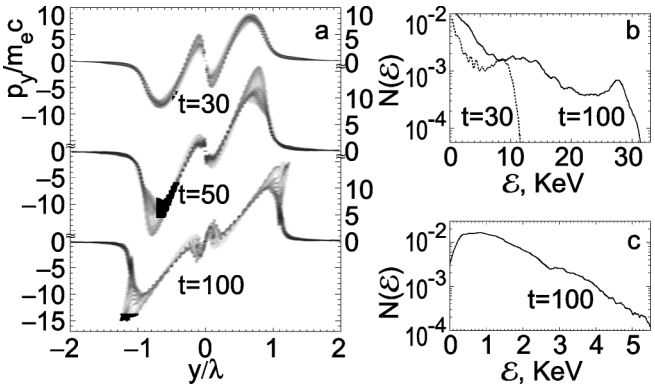

FIG. 5. Ion acceleration during the soliton explosion: (a) the y component of ion momentum, p_y/m_ec, and energy spectrum of ions (b) in the domain [14.3:14.7, −2:2, −0.5:0.5] and (c) in the soliton core [14.3:14.7, −0.5:0.5, −0.5:0.5] at different normalized times ωt.

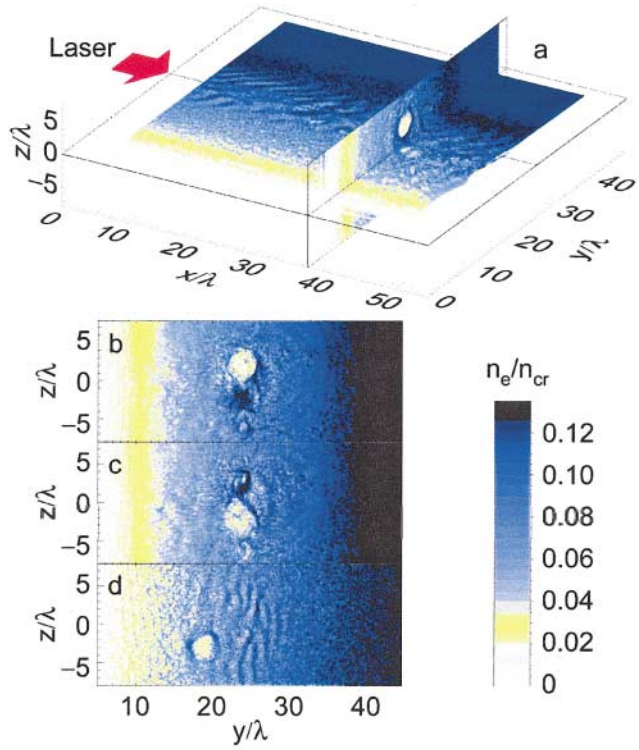

FIG. 6 (color). Three-dimensional view of electron density at $t = 76 \times 2\pi/\omega$ (a), and cross sections of electron density in the y-z plane averaged over the space $35 \leq x \leq 37$ at $\omega t/2\pi = 62.8$ (b), at 64.8 (c), and at 134 (d).

A further proof of the electromagnetic nature of the solitary structure discussed above is provided by the 3D PIC simulation in an inhomogeneous plasma with the density gradient in the y direction from $n_e = 0$ to $0.168 n_{cr}$, as shown in Fig. 6. We show that the soliton can propagate as a whole due to its electromagnetic nature, in contrast to the wakefield that remains at the same place due to its zero group velocity. In this case, the dimensionless amplitude of the incident laser pulse is $a = 3$ and its FWHM size is $5\lambda \times 8\lambda \times 8\lambda$. The size of the plasma slab is $45\lambda \times 43\lambda \times 32\lambda$, and that of the simulation box is $90\lambda \times 48\lambda \times 32\lambda$. Ions are immobile. Initially, the laser pulse propagates along the x axis, its symmetry axis intersects the plasma-vacuum interface at $(x, y, z) = (5, 26, 0)$, where the local Langmuir frequency is $\omega_{pe} = 0.3\omega$. In Fig. 6(a), we see the wakefield and a well-pronounced solitary structure. Frames 6(b) and 6(c) show half a period of the soliton evolution, similar to Fig. 2. Frame 6(d) shows that the solitary wave propagates towards the plasma-vacuum interface against the plasma density gradient. Similar to the 2D case discussed in Refs. [4,14,16], when the soliton approaches the plasma-vacuum interface it radiates its trapped electromagnetic wave away. This result shows clearly the difference between the wakefield and the soliton.

In conclusion, we have demonstrated the existence of the three-dimensional subcycle relativistic electromagnetic solitons in a collisionless cold plasma. The solitons consist of the electromagnetic and electrostatic fields with the structure of the oscillating electric dipole with the poloidal electric field and the toroidal magnetic field confined in the prolate cavity of the electron density. A substantial part of the pulse energy is transformed into solitons, approximately 25%–30% of the incident laser pulse. The core of the soliton is positively charged on average in time, and the soliton undergoes a Coulomb explosion in an ion time scale. This process results in heating of the plasma ions.

We appreciate the help of ILE computer group and CMC of Osaka University (Japan). Two authors (T. E. and S. B.) thank JSPS for their grant. This work was supported in part by INTAS Contract No. 01-0233.

*URL: http://www.ile.osaka-u.ac.jp/research/TSI/Timur/soliton/index.html

[1] V. E. Zakharov, Sov. Phys. JETP **35**, 908 (1972); E. A. Kuznetsov, Chaos **6**, 381 (1996).

[2] B. B. Kadomtsev and V. I. Petviashvili, Sov. Phys. Dokl. **192**, 753 (1970); V. E. Zakharov and A. M. Rubenchik, Sov. Phys. JETP **38**, 494 (1974).

[3] S. V. Bulanov *et al.*, Phys. Rev. Lett. **82**, 3440 (1999).

[4] Y. Sentoku *et al.*, Phys. Rev. Lett. **83**, 3434 (1999).

[5] N. M. Naumova *et al.*, Phys. Plasmas **8**, 4149 (2001).

[6] N. M. Naumova *et al.*, Phys. Rev. Lett. **87**, 185004 (2001).

[7] T. Taniuti and K. Nishihara, *Nonlinear Waves* (Pitman Advanced Publishing Program, Boston, 1983); S. Novikov *et al.*, *Theory of Solitons: the Inverse Scattering Method* (Consultants Bureau, New York, 1984).

[8] K. Mima *et al.*, Phys. Plasmas **8**, 2349 (2001).

[9] T. Zh. Esirkepov *et al.*, JETP Lett. **68**, 36 (1998).

[10] D. Farina *et al.*, Phys. Rev. E **62**, 4146 (2000); D. Farina and S. V. Bulanov, Phys. Rev. Lett. **86**, 5289 (2001); Plasma Phys. Rep. **27**, 641 (2001); S. Poornakala *et al.*, Phys. Plasmas **9**, 1820 (2002).

[11] M. Borghesi *et al.*, Phys. Rev. Lett. **88**, 135002 (2002).

[12] J. M. Dawson and A. T. Lin, in *Basic Plasma Physics*, edited by M. N. Rosenbluth and R. Z. Sagdeev (North-Holland, Amsterdam, 1984), Vol. 2, p. 555; J. M. Dawson, Phys. Plasmas **6**, 4436 (1999).

[13] J. I. Gersten and N. Tzoar, Phys. Rev. Lett. **35**, 934 (1975); V. A. Kozlov *et al.*, Sov. Phys. JETP **49**, 75 (1979); P. K. Kaw *et al.*, Phys. Rev. Lett. **68**, 3172 (1992).

[14] S. V. Bulanov *et al.*, in *Reviews of Plasma Physics*, edited by V. D. Shafranov (Kluwer Academic, New York, 2001), Vol. 22, p. 227.

[15] S. V. Bulanov *et al.*, Phys. Fluids B **4**, 1935 (1992); S. V. Bulanov *et al.*, Plasma Phys. Rep. **21**, 550 (1995).

[16] S. V. Bulanov *et al.*, Physica (Amsterdam) **152D–153D**, 682 (2001).

[17] T. Zh. Esirkepov, Comput. Phys. Commun. **135**, 144 (2001).

[18] A. V. Kuznetsov *et al.*, Plasma Phys. Rep. **27**, 211 (2001); N. M. Naumova *et al.*, Phys. Rev. E **65**, 045402 (2002).